USING FLOW CYTOMETRY TO IDENTIFY KEY CELL POPULATIONS IMPLICATED IN OPIOID-INDUCED OSTEOPENIA IN A CANCER INDUCED BONE PAIN MODEL

By

DIETER MOHAMMAD MOHTY

_____

A Thesis Submitted to The Honors College

In Partial Fulfillment of the Bachelor's degree
With Honors in

Physiology

THE UNIVERSITY OF ARIZONA

M A Y 2 0 1 9

Approved by:

_____

Dr. Todd Vanderah
Department of Pharmacology

Using Flow Cytometry to Investigate Key Cell Populations Implicated in Opioid-Induced Osteopenia in a Cancer-Induced Bone Pain Model

Dieter M. Mohty

ABSTRACT:

Strong opioid analgesics such as morphine are the first line of analgesic treatment for alleviating a variety of acute and chronic ailments. However, prolonged opioid administration causes detrimental side effects. This study investigates one such side effect: chronic peripheral inflammation. To determine whether morphine can exert an inflammatory effect on peripheral tissues such as bone, we created a cancer induced bone pain (CIBP) model. We then constructed an immunophenotyping panel that could identify standard inflammatory and bone degradative populations to see whether morphine can induce the infiltration and proliferation of these cell populations. We also wanted to know if using flow cytometry on treated full femur samples is viable in tracking such populations. Results showed that full femur processing does not impact cell viability and is thus a practical alternative to collect cells for analysis. In addition, we observed some preliminary trends indicating morphine can induce the infiltration of immune and bone degradative cells to the bone marrow. These findings are consistent with previous studies examining orthopedic outcomes of morphine treated patients. This study serves as the foundation for our TLR-4 mediated inflammation hypothesis and will be supplemented with knock-out and biochemical studies in the future.

INTRODUCTION:

Opioids are the first line analgesic treatment for various acute and chronic pathologies including chronic cancer associated pains, post-surgical pain, and general palliation. Opioids are even indicated for other conditions such as diarrhea, fibromyalgia, and musculoskeletal pains (e.g. joint and lower back pain). However, they have many side effects. These side effects are divided into peripheral (constipation, urinary retention, hives, bronchospasm) and central (nausea, sedation, respiratory depression, hypotension, paradoxical hyperalgesia, addiction) [1,2]. Furthermore, recent clinical and basic science studies examining chronic opioid use have shown an increase in bone fragility in both animals and humans [3]. This decline in bone density is especially relevant to women suffering from metastatic bone cancer. Bone is the most frequent site for metastasis. About 70% of metastatic cancers involve bone tissue. Any early-stage breast cancer diagnosis has an appreciable 13.6% chance that it will metastasize to bone within 15 years of the initial cancer diagnosis [4]. Clinicians have observed that patients given chronic opioids attempting to alleviate cancer induced bone pain are more likely to sustain fractures of any kind in the future. This likely prompts the use of more opioids to reduce the subsequent pain which can perpetuate a certainly vicious cycle. Despite the myriad of adverse side effects, opioids are still widely

prescribed. In 2012, over 255 million prescriptions were written. Fortunately, this has decreased to just under 200 million in 2017 [5]. Although there is a steady decline in the number of opioid prescriptions, we are still experiencing the socioeconomic consequences of the ongoing opioid epidemic in the United States. It is clear that opioids' various side effects and potential for abuse heavily mitigate its clinical utility. Therefore, it is important that we explore new approaches to opioid analgesia so that we may develop medications that avoid such debilitating side effects while also providing sufficient pain relief.

One of the standard opioid analgesics prescribed by clinicians is morphine. This compound acts on the μ-opioid receptor (MOR). The MOR is mostly expressed in the central nervous system and to a lesser extent within the periphery. In the CNS, the periaqueductal area (PAG), nucleus reticularis paragigantocellularis (NRPG), and other regions in the limbic midbrain such as the medulla locus coeruleus and caudate nucleus are the primary sites of MOR expression. MOR activation in these regions induces analgesia by inhibiting pain-modulating descending pathways [1,6,7]. In the periphery, MORs are widely distributed among neuronal and non-neuronal tissues such as smooth muscle cells of the GI tract, neuroendocrine cells, and immune cells [1,8]. The MOR, like other opioid receptors, is G-protein coupled receptor (GPCR). Activation by an agonist such as morphine triggers the common downstream inhibitory pathway of most GPCR(αi)s. The heterotrimeric G-protein dissociates into Gα and Gβγ, both of which have functional downstream effects. The Gα subunit binds to and activates Kir3, an inward-rectifying potassium-channel [1,8]. Gα also downregulates cAMP production by directly inhibiting the activity of adenylate cyclase. Gβγ binds and inhibits various voltage-gated calcium channels [6,8]. In addition, the reduction of cAMP further inhibits calcium influx as cAMP-dependent calcium influx channels are inhibited as well. Ultimately, the modulation of these channels reduces the excitability of neurons and the release of the neurotransmitter GABA, directly inhibiting pain transmission. Receptor activation is reversed by GTPase, which is activated upon the binding of Gα to its downstream targets such as Kir3. Once GTP is hydrolyzed to GDP, Gα becomes functionally inactive and reforms with Gβγ to become the inactive heterotrimeric G-protein, ready for subsequent reactivation [1]. This signaling cascade is conserved between peripherally and centrally expressed MORs.

There is also substantial evidence that morphine is able to agonize toll-like-receptors (TLRs), specifically the TLR-4. TLRs are a family of receptors unique to innate immune functioning. Their purpose is to recognize defined molecular patterns associated with pathogens or with cellular damage. The TLR-4 is one such receptor found on cells from the myeloid lineage, including macrophage and its various derivative cells such as dendritic cells and osteoclasts [9,10]. Normally, the TLR-4 is agonized by bacterial lipopolysaccharide (LPS). Stimulation of the TLR-4 leads to the activation of the NFκB pathway. This pro-inflammatory pathway leads to the production of inflammatory cytokines such as TNF-α, IL-1, IL-6, among other markers [10]. Interestingly, various studies have observed that short-term administration of morphine and its derivative metabolite morphine 3-gluconirde can sufficiently agonize the TLR-4 [11]. In relation to osteopenia, whether that be a result of metastatic bone cancer or other pathologies such as rheumatoid arthritis, the use of strong opioid analgesics has been observed to negatively impact clinical outcomes [12]. We hypothesize that morphine's ability to agonize the TLR-4 would further prolonged inflammation by recruiting inflammatory cell populations to the already inflamed site. Therefore, we would expect that morphine would further worsen long-term outcomes for people with metastatic bone cancer due to continuous inflammation of bone tissue. To understand exactly how this inflammatory process can lead to osteopenia and an increase in the risk for lesions or

fractures, it is important to understand the basics behind osteoclast differentiation and proliferation.

Osteoclasts (OCs), or "bone resorbing cells", play a pivotal role in bone development, remodeling, metabolism, and bone homeostasis. OCs, like other myeloid cells, originate from hematopoietic stem cells (HSCs) and differentiate from the monocyte/macrophage lineage. From the bone marrow, HSCs differentiate to common myeloid progenitors (CMPs) upon binding IL-3 and IL-6. CMPs differentiate into granulocyte/macrophage progenitors (GMPs) after stimulation from GM-CSF. Then, M-CSF sustains and differentiates GMPs into monocyte/macrophage-like cells, or OCPs [13]. Finally, RANK-L induces osteoclastogenesis from OCPs. It is believed that peripheral monocytes and other precursor cells are directly recruited to "bone remodeling compartments" (BRCs) via penetrating capillaries. It is also thought that these compartments provide the ideal environment for osteoclastogenesis to occur.

M-CSF, or CSF-1, is a growth factor and cytokine secreted by various musculoskeletal cell populations. In the context of initiating osteoclastogenesis, osteocytes have been observed to be the main driving force in the production of M-CSF despite osteoblasts and stromal cells' dominance in producing and secreting this cytokine [13]. Osteocytes produce M-CSF upon experiencing mechanical stress or microdamage. The release of this cytokine acts to recruit precursor cells (generally monocytes or macrophages) to initiate osteoclastogenesis. There is no consensus on the mechanism of recruitment into the bone microenvironment, but researchers hypothesize it is a combination of M-CSF and other markers related to stress and microdamage that permanently recruits these precursors to BRCs. M-CSF binds to c-fms (CD115), a tyrosine kinase receptor found on GMPs and OCPs. Binding of M-CSF to c-fms results in receptor dimerization and autophosphorylation of select tyrosine residues. Intracellularly, the resulting ERK and PI3K/Akt cascades leads to transcriptional upregulation of genes which ultimately results in the proliferation and survival of OCPs. [13,14].

RANK-L is a cytokine from the TNF-α family. RANK-L acts on the RANK receptor, otherwise known as the NFκB receptor. This cytokine is crucial in normal bone remodeling and osteoclastic activity. This ligand is notably expressed in marrow stromal cells (MPPs), B-cells, T-cells, and osteocytes. Like M-CSF, RANK-L production is a primarily osteocyte mediated process. However immune cells can drive OC development in states of chronic inflammation [15]. This cytokine is expressed as a membrane bound protein or a secreted protein. Secretion or RANK-L requires proteolytic cleavage via matrix metalloproteases [16]. The RANK receptor is generally expressed on late precursor and fully differentiated osteoclasts. RANK-L binding to the RANK receptor recruits TNF receptor associated factors, or TRAFs (notably TRAF6), to the intracellular domain of the receptor. This induces NFκB expression, which acts on the nucleus to upregulate osteoclastic genes such as NFATc1 [13,16]. Activation of NFATc1 initiates many osteoclastic activities, such as attachment and formation of a ruffled border. However, this can only happen in the presence of M-CSF. Interestingly, RANK-L has also been observed in directly inducing osteoclastogenesis from macrophage lineage cells and that OCPs not exposed to sufficient levels of RANK-L will differentiate into macrophages [13,17,18]. Although cytokines such as TNF-α and IL-1/IL-1β can induce osteoclastogenesis, differentiation only occurs in the presence of RANK-L [13,19]. This is because RANK-L induces the production of cognate receptors to these inflammatory cytokines and essentially "primes" cells for osteoclastogenesis. The observations that TLR-4's activation produces many of these described cytokines provides further evidence that morphine may be able to indirectly exert osteoclastogenic effects on the bone [11,16].

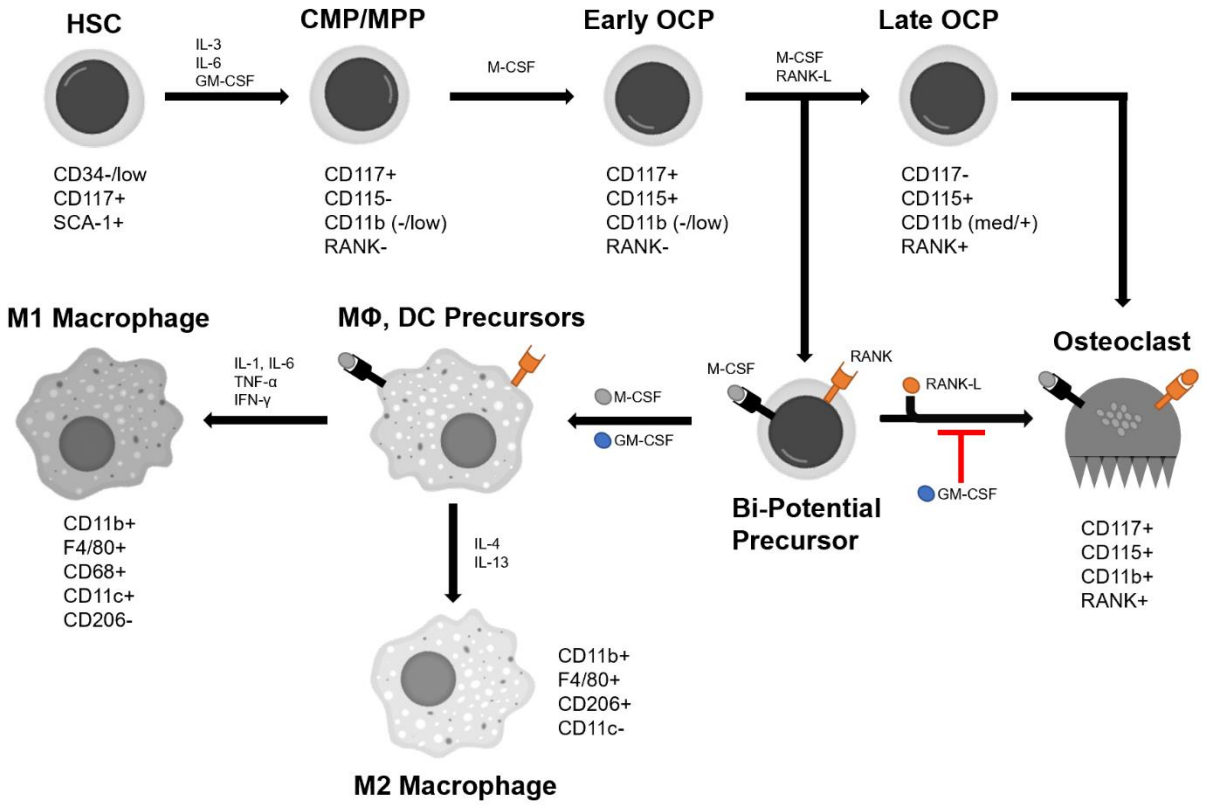

Figure 1A (Above): A basic schema demonstrating the relationship between various myeloid cell types. This schematic also describes key cytokines involved in the development of these cell types. Not included are monocytic cells, which also come from the common myeloid progenitor cell (CMP).
Adapted from Miyamoto et. al [17,23]. Images sourced from Mikael Häggström, Wiki Commons.

Normally, bone homeostasis and healing are harmonized efforts between osteoblasts and osteoclasts. An imbalanced ratio of osteoclast to osteoblasts populations will lead to bone loss and osteopenia. Although the recruitment of inflammatory cells is required in normal bone healing, it is an acute inflammatory state. In relation to bone healing, an acute inflammatory state is required to facilitate the recruitment of precursor cells so that they may differentiate into osteoclasts to initiate the remodeling process. However, a chronic inflammatory state impedes the healing process **[15,18]**. Thus, it is important to determine how morphine administration may contribute to this state of prolonged inflammation in this cancer induced bone pain model (CIBP). It is also important to consider the burden cancer has on bone in this model. Bone metastases are particularly devastating due to the degradative effects that tumor cells exert on bone microenvironment. Circulating tumor cells (CTCs) that reach the bone are able to undergo mesenchymal-to-epithelial transformation. This process results in the release of various peptides such as parathyroid hormone related protein (PTHrP) that induce osteoblasts and osteocytes to upregulate RANK-L production **[4,20]**. So, the damage caused by tumor growth and the resulting immune response to the tumor is further compounded by the recruitment and activation of inflammatory populations to the microenvironment. Because both TLR-4 activation and bone metastases can upregulate the production of many of these cytokines, this provides further evidence our theory that opioids are

able to shift the equilibrium of homeostatic bone remodeling towards pathological amounts of bone degradation by promoting osteoclastogenesis and the recruitment of inflammatory cells.

Based off these observations and relationships, we hypothesize that morphine's ability to agonize inflammatory receptors such as the TLR-4 ultimately results in bone degradation and impeded bone healing, both of which are risk factors for future fracture(s). We suggest that the recruitment of peripheral and stromal myeloid populations which differentiate into inflammatory macrophages and bone-resorbing osteoclasts contributes to this observed phenomenon. The overall objective of this project is to determine whether (and to what extent) morphine exerts an inflammatory influence on the bone microenvironment. To achieve this, we will attempt to use fluorescence assisted cell sorting (FACS) analysis on full treated cancer and non-cancer femur samples. Ideally, we will be able to identify and measure frequency changes of various cell populations that may infiltrate the bone with respect to treatment. However, the described study can only provide indirect evidence to a TLR-4 mediated inflammatory effect, so this study will need to be supplied with TLR-4 KO studies to verify that TLR-4 is the mechanism behind our observations. In addition, follow-up investigations into how alternative analgesics and combinations of endocannabinoids and opioids may mitigate this proposed phenomenon will be explored.

KEY WORDS: Opioids, Mu-opioid receptor (MOR), Toll-Like-Receptor, CIBP, Peripheral Inflammation, Macrophages, Osteoclasts, Osteopenia.

METHODS:

Mice: Female mice aged 7-8 weeks from a C57BL/6J background were purchased from Jackson Laboratories. All mice were housed at the University of Arizona's animal facility. Upon arrival, mice were allowed to acclimate for seven days prior to any procedures. All procedures were approved under The University of Arizona's IACUC protocol #06-110. Euthanasia was performed via cervical dislocation after ketamine/xylazine anesthesia. For this study, mice were grouped into the following treatment groups: Naïve (Baseline), Sham Surgery + Saline (SS), Sham Surgery + Morphine (SM), Cancer Surgery + Saline (CS), and Cancer Surgery + Morphine (CM). Each group contained an N = 5 for a total of 25 animals.

Antibody Panel: We constructed a twelve-antibody panel containing the following antibodies and conjugations: CD3 (A700), CD19 (A700), NK1.1 (A700), CD11b (BV570), CD11c (BV650), CD68 (PeCy7), CD115 (APC), CD117 (BV421), CD206 (BV711), RANK (PE), F4/80 (APC Fire 780), and Live-Dead (PE TXR). This allowed us to identify macrophage/monocyte lineage cells, osteoclast precursors (in various developmental stages), osteoclasts, and M1 and M2 polarized macrophages. This panel is based off surrounding literature describing relevant markers in bone and in other related lymphoid organs [21-25, 33].

***Breast Cancer Cell Culturing*:** To develop a syngeneic metastatic breast cancer model, EO771 adenocarcinoma cells were grown in Dulbecco's Modified Eagle Medium (DMEM total medium) with 10% Fetal Bovine Serum (FBS), 1% penicillin/streptomycin and 25mM HEPES

buffer. Cells were passaged (1:10 dilution of cells into new media) every four to five days to ensure viable cells were readily available for cancer surgeries and for other in-vitro studies.

***Intrafemoral Inoculation*:** Mice undergoing interfemoral inoculation (sham or cancer treatment) were anesthetized with ketamine/xylazine (90mg/kg//10mg/kg i.p). Right and left femurs were imaged using a micro CT X-ray imager. A small incision was created above the right leg. This opening was then expanded to visualize the fascia and muscles surrounding the femur. By removing the surrounding fascia and separating the vastus lateralis from the rectus femoris we could sublux the knee and expose the distal femoral condyles. We then bored a hole into the medullary canal of the femur. A placeholder rod was inserted and the femur was X-rayed again to verify the integrity of the femur. Using a Hamilton microinjector, we injected approximately 80,000 E0771 cells (5μL) into the medullary canal. Sham animals received 5μL of media only. The hole was sealed with bone cement and the knee was readjusted to its prior position. The skin incision was then stapled together.

Behavior Testing & micro-CT: Behavior was tested on day 7, 10, and 14 for verify tumor burden and pain. Treated animals were tested for flinch and guard responses on minute intervals. Additionally, we observed functional leg use and weight-bearing activity to verify animals were not in extraordinary pain. If so, they were excluded from the study. Both contralateral and ipsilateral femurs were x-rayed on day 0, 7, 10, and 14 to evaluate bone quality over time. Bone quality was assessed using an in-house 'bone scoring' report. (See Figure 2 for scoring criteria)

Osmotic Minipumps: Starting at day 7, all surgerized mice were given subcutaneous osmotic minipumps containing either saline or morphine. Mice were anesthetized with 0.1mg/kg xylazine/ketamine. A small subcutaneous incision was made on the upper back. The incision was then expanded to fit the osmotic minipump. The osmotic minipumps had a drug delivery rate of 10mg/kg/day. Drug administration continued until day 14.

Sample Preparation: On day 14, mice were anesthetized, x-rayed, and sacrificed via by cervical dislocation. Full contralateral and ipsilateral femurs were collected, cleaned, and placed in microcentrifuge tubes containing cold RPMI media. Individual femurs were then placed in FACS buffer and grinded with a ceramic pestle and mortar. The resulting suspension was strained through a 70μm cell strainer five times to exclude bone fragments and other debris. The run-through collected into 50mL tubes. All samples were then centrifuged at 2000RPM for 5 minutes. After removing excess media, the pellets were resuspended using 200μL FACS buffer (PBS with 2% FBS). 150μL of each sample was transferred to a 96-well plate, with the remaining 50μL allocated to create pooled samples for full-minus-one controls (FMOs). All samples were stained and run through the LSRFortessa flow cytometer no more than 12 hours after sample preparation to maximize cell viability and antibody conjugation stability.

Immunofluorescence Staining: 50μL of Fc-Inhibitor solution (a 1:50 1μL FC-block in 50μL FACS) was added to each sample to prevent nonspecific binding. The Fc-block incubated for 15-20 minutes. Thereafter, samples were stained for surface markers with 50μL a prepared antibody solution. The solution was a 1:50 dilution of each antibody (CD3, CD11b, CD11c, CD19, CD115, CD117, CD206, NK1.1, F4/80) in FACS buffer. FMOs were created for the following

antibodies: CD11c, CD68, CD115, CD117, CD206, and RANK. Samples were then allowed to incubate for 45 minutes at 4°C. Samples were then washed with 100μL PBS and were then centrifuged for 3 minutes at 2000RPM. (Note: A "wash" step includes resuspension, centrifugation, and removal of excess media.) This wash was repeated with 100μL PBS/well. Following the second wash, each well was incubated with 100μL solution of a 1:1000 dilution of Live-Dead viability dye. After another 30-45-minute incubation, the cells were washed with 100μL PBS/well and then fixed with 200μL/well of BD Cytofix solution. This was allowed to incubate for 5-7 minutes. Samples were then washed with 200μL/well FACS buffer. After removing excess FACS media, a 100μL of a 1:10 dilution perm-wash in dH_2O was added to each sample. The samples were then washed three times using 100-200μL/well of perm-wash. Cells were then stained intracellularly using a 1:50 dilution of CD68 in perm-wash solution, with 50μL pipetted per sample. After another 30-45-minute incubation, cells were washed with 100μL and then 200μL/sample of perm-wash. After removing the excess media, a 1:5 dilution of count beads in FACS buffer (500μL beads in 2000μL FACS) was prepared. Each sample was resuspended using 50μL of the count bead solution. Single color compensations were made using a 1:15 dilution of compensation beads (concentration of 10500 beads/μL) in FACS buffer. For every antibody used, a microfuge tube containing 100μL of the compensation bead solution was prepared. 1μL of antibody was pipetted into its respective microfuge tube We compensated Live-Dead using Anti-human granzyme B (GzB) as it fluoresces in the same wavelength (PE TXR). This is because the compensation beads can only bind antibodies and the Live-Dead stain is not an antibody. For the triple negative channel (CD3/CD19/NK1.1 with A700 conjugation), 1μL of each antibody was pipetted into a single microfuge tube. Rainbow beads were used before each run to verify laser and voltage consistency between runs. Data collection was standardized to the collection of 2500/5000 count beads, depending on overall cell viability.

Analysis of Flow Cytometry and Bone Scoring Data: FACS data was compiled and analyzed using FlowJo V10 and PRISM. Cell counts and frequencies for populations of interest were compared across treatment groups. Bone scoring was done based off an in-house scoring scheme. The bones were rated on a scale from zero (unremarkable) to four (bi-cortical fractures and severe lesions). Bone quality was scored in a blinded to treatment fashion for images taken on day 0 and on day 14. Scores were then averaged across three independent raters.

DATA:

Bone Scoring: Several reports, including preliminary data from our lab, suggest that morphine exerts an inflammatory (and thus destructive) effect on the bone microenvironment. X-rays provide visual proof to such effects our described treatments may have. To find significance between groups, we created a semi-qualitative scoring system that would allow us to report differences numerically. Day 0 and day 14 femurs were then compared to each other to best visualize differences in bone quality and density with respect to treatment. We did not incorporate day 7 and day 10 images in our studies. This is because E0771 adenocarcinoma cells don't proliferate significantly until day 14. The results with representative images from each group are shown below.

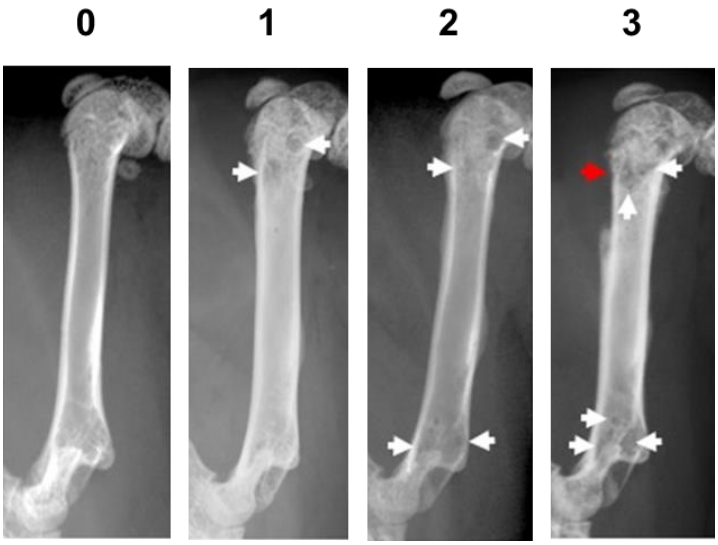

Figure 2 (left): *The semi-qualitative bone scoring system. White arrows represent lesions and red arrows represent cortical fractures*

0 = Normal Bone

1 = One to three lesions

2 = Four to six lesions

3 = Uni-cortical bone fracture

4 (not shown) = Bi-cortical bone fracture

Figure 3 (right): Representative images for day 14 bones by treatment. All femurs shown are ipsilateral (right) sided.

(A) is a naïve (untreated) bone.
(B) is a sham + surgery mouse.
(C) is a sham + morphine mouse.
(D) is a cancer + saline mouse.
(E) is a cancer + morphine group.

Notice where the inflammatory and osteoclastic activity is concentrated. This observation is interesting as the E0771 cells are injected into the medullary canal of the bone itself.

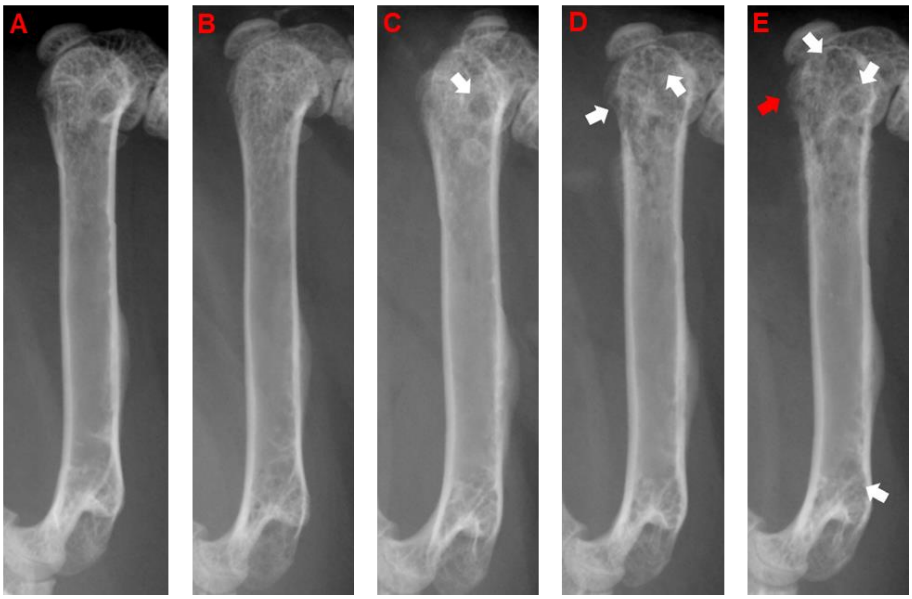

From these x-ray images it appears that inflammatory and osteoclastic activity leading to bone loss occurred almost exclusively in the trabecular bone of the proximal and distal ends the femur. There was limited activity in the diaphysis of the femurs. Looking at (C) and (E) we see that the administration of morphine is implicated with the formation (or worsening) of lesions and the development of metaphyseal fractures. We did not see any bicortical fractures in any treated femur.

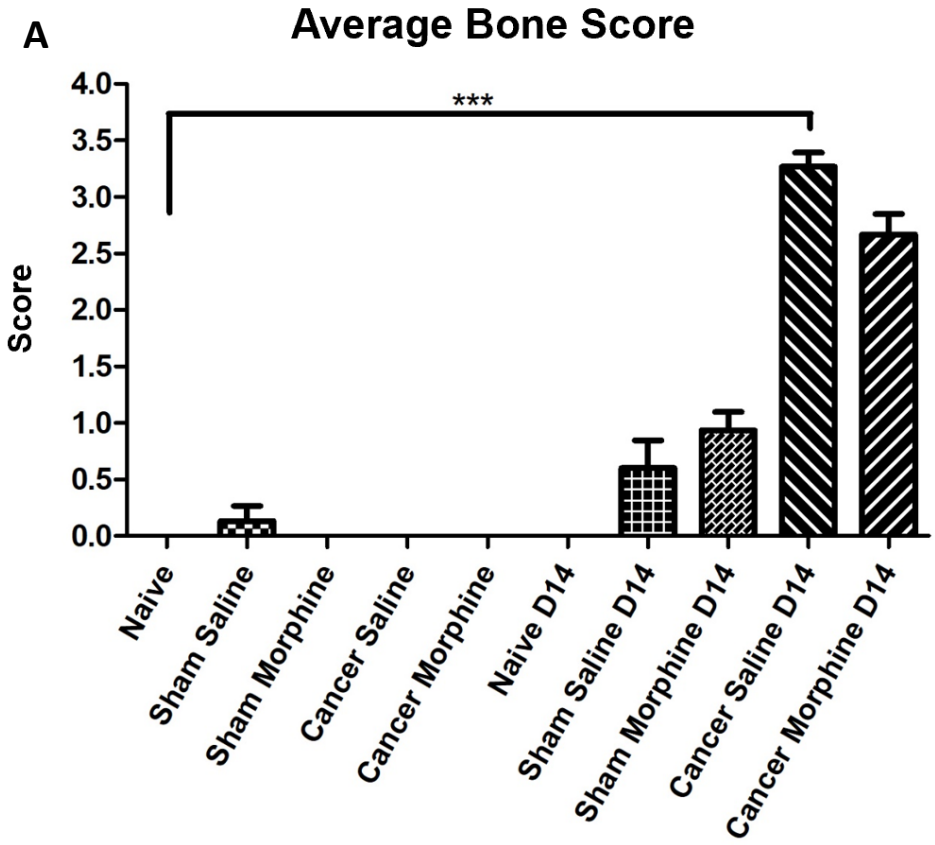

Figure 4A (left): The average score from three independent scorers by treatment. Although we have data that shows a significance between cancer morphine (CM) and cancer saline (CS) at day 14, the results from this particular set (N=5) indicates little significance.

This was later determined to be due to high variability from the experimental parameters exacerbated by a low N-value

FACS - Preliminary Gating: All data collected was analyzed using FlowJoV2. We gated for live cells using our Live Dead stain against histogram. From this live population, we gated on SSC-A vs FSC-A to visualize proliferating lymphocytes. We then gated the lymphocyte populations against our triple negative CD3/CD19/NK1.1 gate. This allowed us to exclude B-cells, T-cells, and NK-cells. After these initial gates, we looked into various populations of interest.

M0 and M1 Polarized Macrophages: We gated triple-negative cells against F4/80 and CD11b and took double positive cells. From $CD11b^{+}$ $F4/80^{+}$ group we could look at M1 and M2 polarized macrophages as our immunophenotyping panel included CD11c, CD68, and CD206. The identification of M1s generally requires two distinct markers. We determined $CD11c^{+}$ and $CD68^{+}$ cells were M1 macrophages. We determined M2s as $CD206^{+}$ $CD11c^{-}$.

Myeloid Cell Linage Populations: We identified myeloid cells by gating on CD115 and CD117 after looking for varied expression of CD11b. We determined OCPs to be $CD11b^{-/low}$ and late precursors as $CD11b^{mid/+}$. We visualized CD11b low expression with a histogram, which showed two distinct peaks of fluorescence. Looking at CD117 and CD115 expression, we saw four distinct populations: $CD117^{-}/CD115^{-}$, $CD117^{+}/CD115^{-}$, $CD117^{-}/CD115^{+}$ and $CD117^{+}/CD115^{+}$. We considered intermediate CD117 levels to be positive. We determined the double positive cells are late OCPs or early OCs) The $CD117^{+}/CD115^{-}$ population was determined to be progenitor cells. Although identifying progenitors in this manner is likely inaccurate, they provided some insight into the proliferative activity of cells.

Figure 5A-K: Gating Scheme for Full Femur Samples

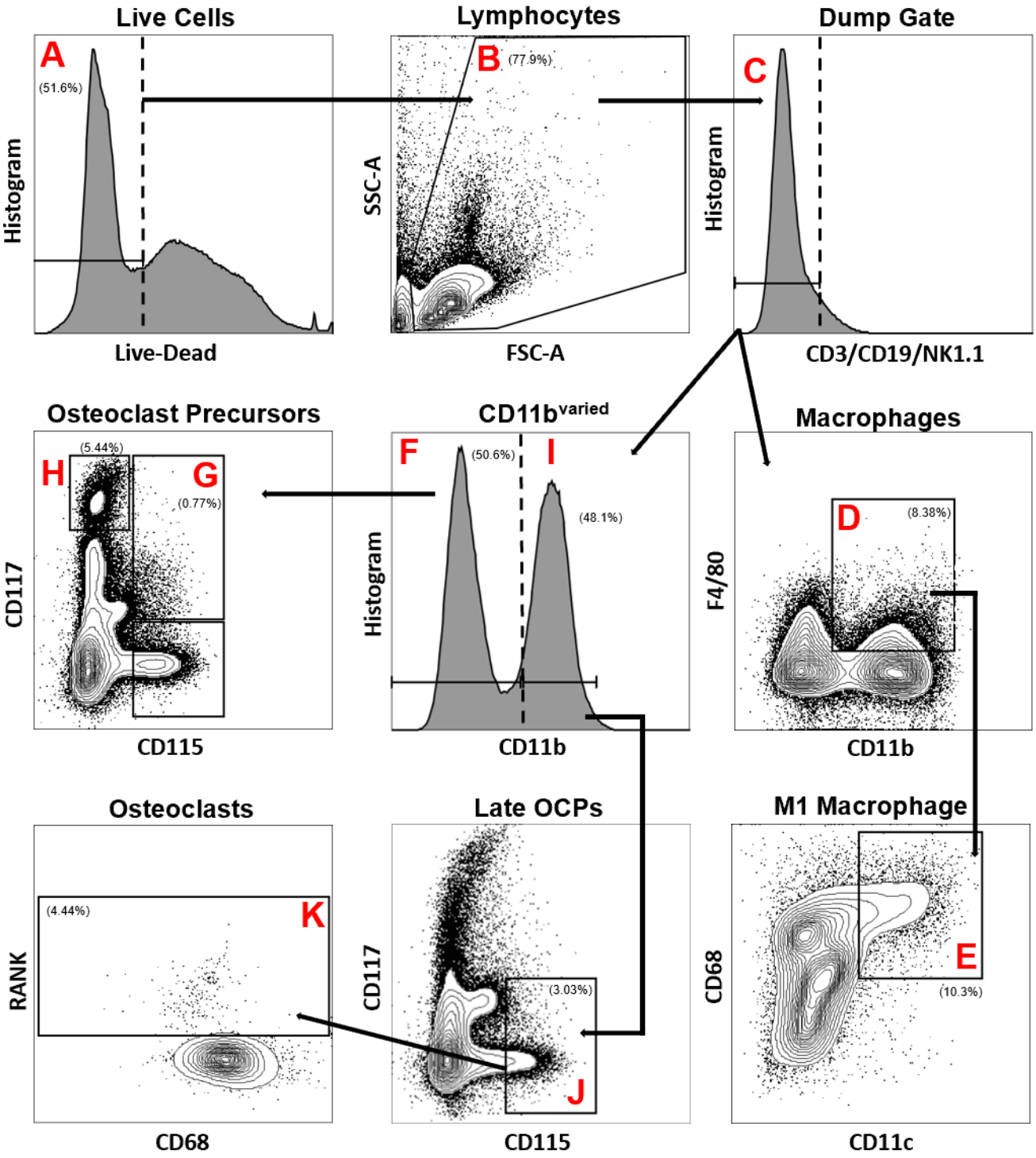

The following cell types described are: **(A)** Live Cells **(B)** Proliferating lymphocytes **(C)** B-cell, T-cell, NK-cell dump **(D)** Macrophage (M0) **(E)** M1 Macrophages **(F)** CD11b^{low} precursors **(G)** Early OCPs **(H)** MPP/CMPs **(I)** CD11b^{+} late precursors **(J)** CD115^{+} CD117^{-} Late OCPs **(K)** RANK^{+} OCPs and OCs

From the gating scheme and antibody panel described above we attempted to identify five populations of interest: macrophages, M1 polarized macrophages (not shown), early progenitors, osteoclast precursors, and osteoclasts. We applied the above gating scheme to each cell population of interest to see if morphine exerts an inflammatory effect on the bone microenvironment.

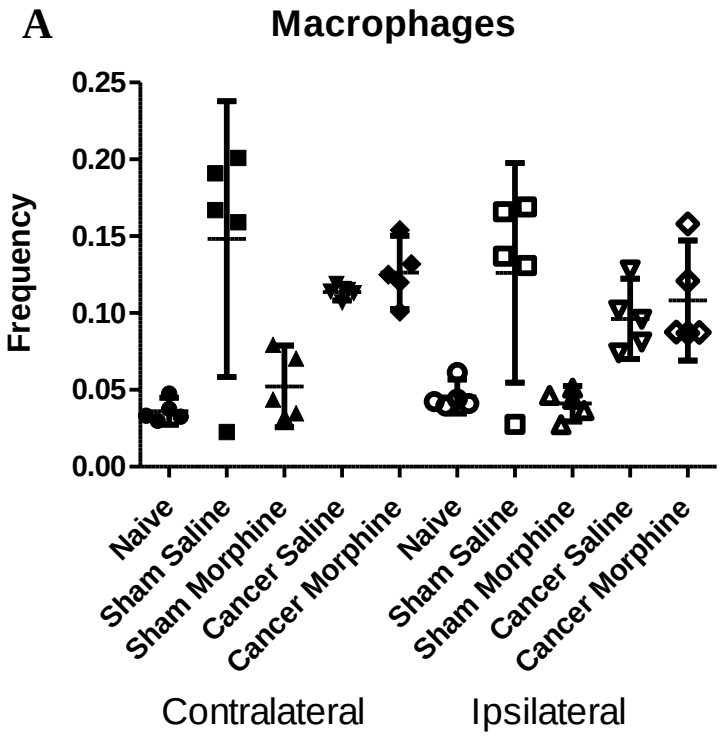

Figure 6A: Frequency counts for undifferentiated macrophages. This set is represented by **(D)** in the gating scheme above, which is gated off the Live, TN, $CD11b^{+}$ $F4/80^{+}$ gates.
The sham surgery + saline group has near-outlier points in both contralateral and ipsilateral sides.

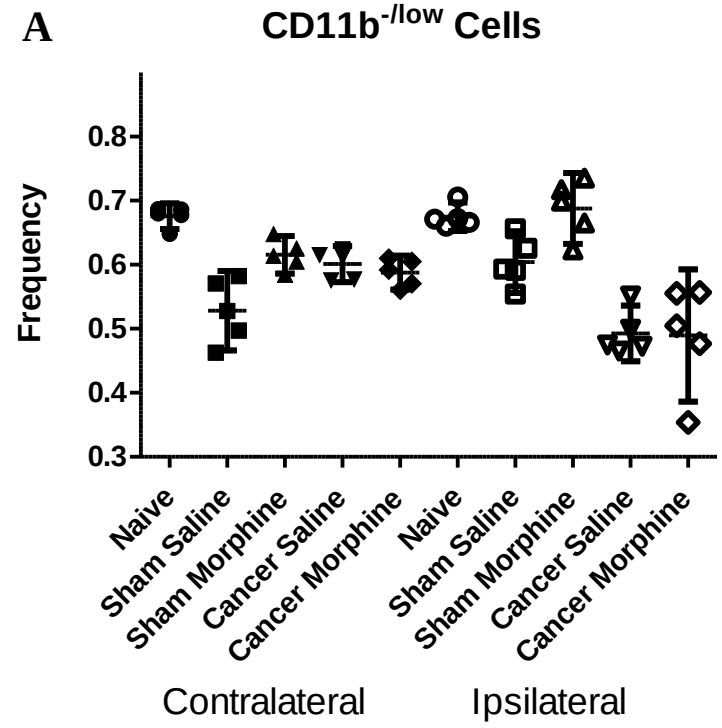

Figure 7A: Frequency counts for early myeloid cells, broadly referred to as Live, TN, $CD11b^{-/low}$ cells. This set is represented by **(F)** in the gating scheme above.

This trend reverses when plotting $CD11b^{mid/+}$ cells (cells represented by Figure 5I, data not shown).

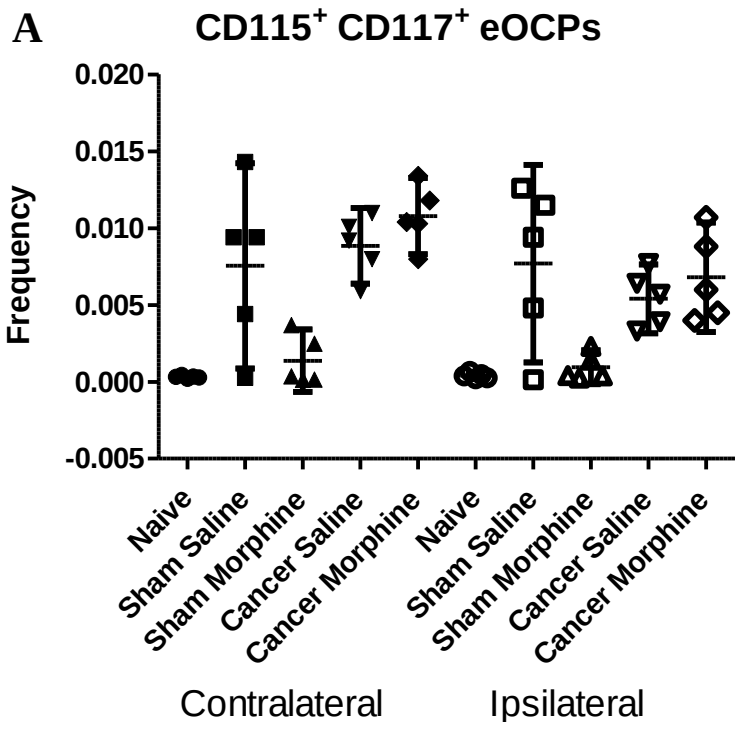

Figure 8A: Frequency counts for early osteoclast precursor cells. This set is represented by **(G)** in the gating scheme above, which is gated off the Live, TN, $CD11b^{-/low}$ $CD115^{+}$ $CD117^{+}$ gates. The sham surgery + saline group has near-outlier points in both contralateral and ipsilateral sides.

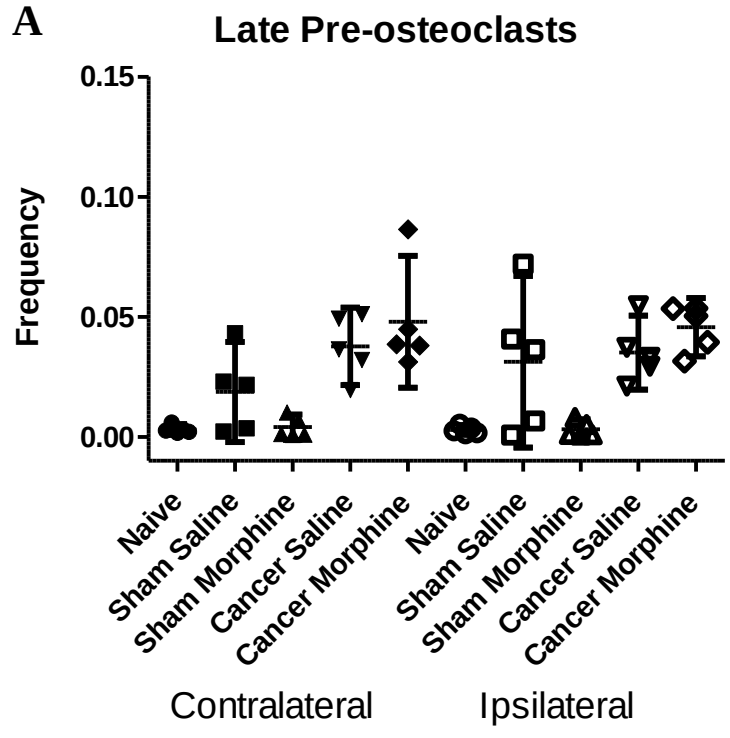

Figure 9A: Frequency counts for late stage osteoclast precursors. These were gated from Live, TN, $CD11b^{mid/+}$ $CD115^{+}$ $CD117^{-}$ cells. This set is represented by **(J)** in the gating scheme above.

RANK positivity increases when compared to $CD11b^{low}$ $CD115^{+}$ $CD117^{-}$ cells.

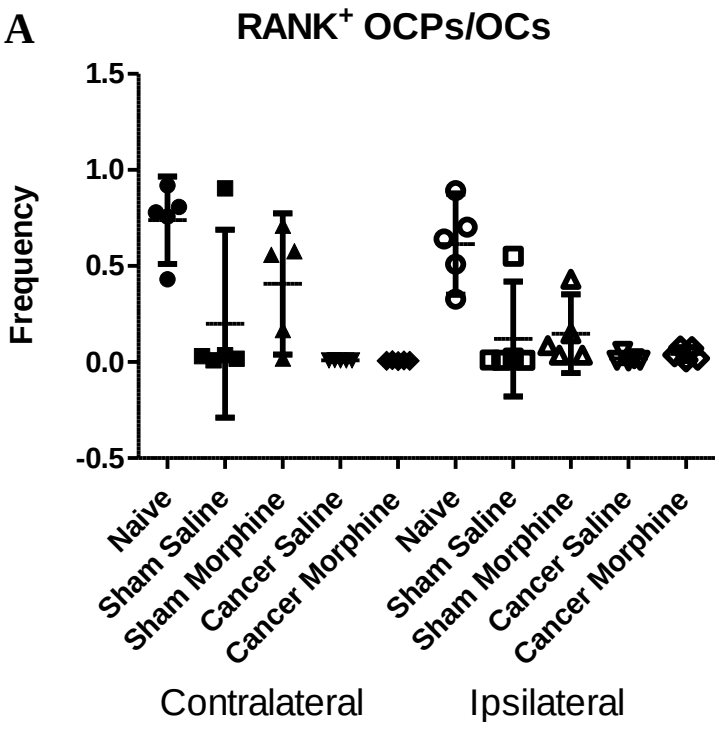

Figure 10A: Frequency counts for RANK+ OCPs and OCs. This set is represented by **(K)** in the gating scheme above, which is gated off the Live, TN, $CD11b^{mid/+}$ $CD115^{+}$ $CD117^{low/-}$ $RANK^{+}$ gates.
Unfortunately due to the extreme variance between groups, we cannot make any determinations with RANK+ OCP/OCs

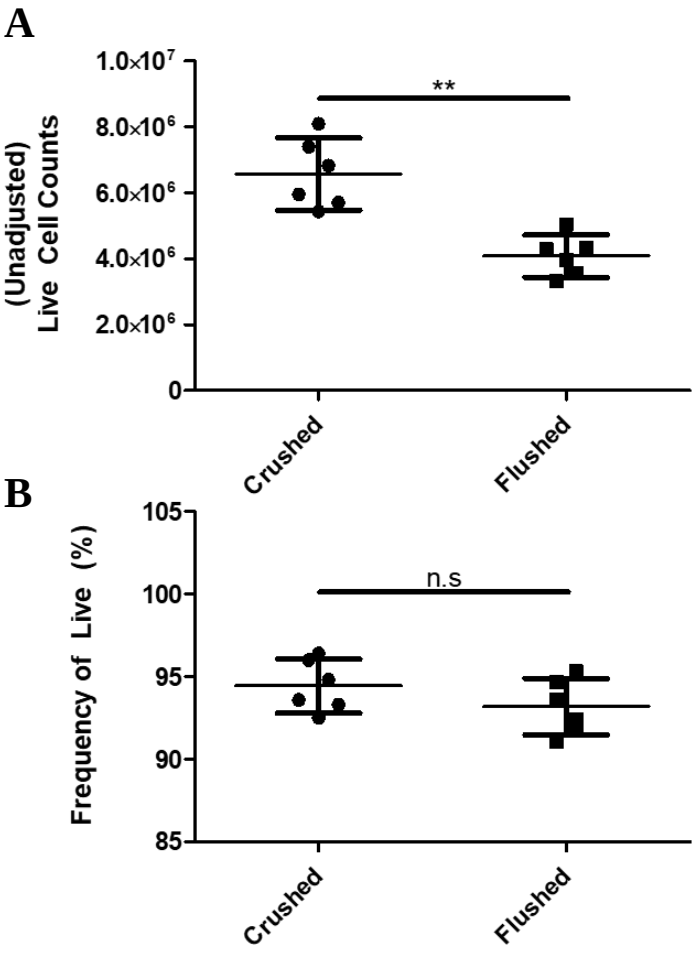

Figure 11A & 11B: Comparing the absolute (unadjusted) count and frequency of live cells in naïve animals when testing the traditional "flushing" method vs "crushing" and processing whole femurs (N=6)

Note: Live-cell frequencies were calculated only for naïve femurs. However, we believe that there will be no significance in viability between the two methods for any given treatment.

DISCUSSION:

In this study we demonstrate flow cytometry using full femur samples is a viable method in cell counting bone and bone marrow populations. Traditional bone marrow studies gather cells via flushing the bone marrow cavity out. This is done by cutting the proximal and distal ends of the femur off so that a needle can be inserted to wash out bone marrow contents [25,26]. Based off the x-ray images of bones from this study, we see that osteoclastic activity is concentrated in the distal and proximal ends of the femur. So, excluding these areas of high activity could misrepresent tangible changes occurring in the bone. By showing that full femurs can be analyzed with flow cytometry, we can better examine the overall effect our treatments may have on the bone. However, there are a few concerns that need to be addressed before incorporating this "crushing" method into future experiments. Firstly, there is a potential problem with cell viability. This relatively violent method in extracting cells (crushing with a pestle and mortar and straining through a 70-micron filter) might kill a lot of cells. When comparing the two methods, we found no significance in viability (92-97%, naïve femurs, N=6, Figures 11A & B, no data for treated femurs). However, the overall viability does not mean that specific cell populations of interest are not affected. This is especially the case with rare populations such as osteoclasts. This is because they are in such small proportion as to not significantly impact overall viability. In addition, the massive increase in overall cell populations may mitigate any significance in cells of interest, but this is easily controlled with a highly specific and sensitive panel and conducting analyses using frequencies instead of absolute counts.

There is a consensus among researchers that osteoclast precursors express varying levels of CD115 (M-CSFR) and CD117 (c-kit), depending on the stage of maturation and differentiation [22,23]. In addition, we defined early precursors that were highly enriched for osteoclastic potential as TN^{-} $CD11b^{-}$ $CD115^{+}$ $CD117^{+}$ [15,17,22]. Such populations are generally dissected after looking at CD11b expression. The $CD11b^{-/low}$ early myeloid precursor cells showed an interesting trend. Because CD11b expression is upregulated as these cells differentiate into late OCPs and OCs, we can indirectly figure the shift towards osteoclastogenesis by looking at decreases in $CD11b^{-/low}$ populations [22]. Cancer animals showed a significant decrease in the frequency of $CD11b^{-/low}$ cells which was further decreased with morphine administration. This observation indicates a myeloid/osteoclastogenic or even increased monocyte/macrophage infiltration in the bone. This downward trend in $CD11b^{-/low}$ was reversed when we looked at $CD11b^{mid/+}$ expression levels, in which we saw increases in cells that had medium to high expression levels of CD11b (Figure 5J). This observation was followed further into the CD115 CD117 gating, where we found a significant shift towards mature osteoclast precursors. This can be visualized when comparing the frequency of CD115+ CD117- cells in Figure 5J to the CD115+ CD117- cells derived from the $CD11b^{low}$ gate. In Figure 5J, we can see a clear shift from CD115 negativity to CD115 positivity with a decrease in CD117 expression (so a shift from CMP-like populations to OCPs). This can be seen by the development of a 'notch' just outside the (J) Gate. This observation of osteoclastic maturation is consistent with papers such as Jacquin et. al, where they demonstrate that as OCPs mature, they downregulate CD117 and upregulate CD11b [22]. This also follows suit with the consensus that "committed" OCPs express CD11b, CD115, RANK, but not c-kit [23]. It is important

to note that these conclusions are predicated on the assumption that CD115- CD117+ can be considered as proliferating CMPs (or early progenitors).

Early precursors do not express RANK receptor positivity. We confirmed this by looking at the subset of early osteoclast precursors expressing $CD117^{+}$ $CD115^{-}$. We found that an overwhelming majority (>99.5%) of cells in this set did not express the RANK receptor. As late OCPs mature into early OCs, they begin to express varying levels of the RANK receptor. However, identifying maturing and fully mature/active osteoclasts using the RANK receptor was largely ineffective and so we could not make any determinations on osteoclast frequencies. The variability in RANK positivity can be attributed to a variety of issues. One issue could be the weak staining of RANK is either due to the parameters of the experiment or that the antibody fluoresces extremely weakly. However, the conjugation for RANK receptor antibody was in the PE channel, (a channel that is not susceptible to auto-fluorescent issues) and so it is likely due to another reason. We believe that this specific antibody is not particularly good for determining RANK positivity.

Our macrophage identification and frequency counts had variable success. Undifferentiated macrophages (MΦs) and M1 macrophages generally gave good frequencies. Unfortunately, looking for M2 macrophages using CD206 proved ineffective. Gating with CD206 showed insignificant population counts/frequencies across all groups and treatments and so analysis using CD206 was excluded. Many researchers consider CD206 to be an M2 macrophage specific marker. Recent literature surrounding suggests otherwise, as CD206 is expressed on various other cells included but not limited to macrophages and dendritic cells **[21,25,28]**. Furthermore, CD206 expression is low in M2s compared to other potential M2 markers, despite CD206 recognition as an M2 specific marker **[28]**. Identification of M1 polarized macrophages generally requires two distinct markers due to shared expression of many macrophage-associated markers. So, gating CD11c with CD68 allowed us to identify such macrophages fairly well. However, monocytes also express similar markers which makes sense as they very closely related. Like with our OCP populations, we found a similar trend forming with MΦs. We observed a significant increase in macrophages frequency which was further increased with morphine administration in both cancer and non-cancer animals. This observation indicates an increased monocyte/macrophage infiltration in the bone. It is important to note that this determination was made with the exclusion of our sham + saline group (which was giving us exceptionally variable counts with most other populations we studied).

The FMO for CD117 gave us some difficulty. We ended up being more conservative in defining $CD117^{-}$ cells because there was a lot of bleed-through in the BV421 channel. We are still unsure of what may have caused this. We do know it is not due to the inherent granularity of cells (this generally occurs in 475-500nm), compensation, or spectral overlap. So, for the purposes of our analyses, we were more lenient in what constituted $CD117^{low/mid}$. However, we were able to easily identify $CD117^{+}$ as our groups gave a distinct and concentrated population, as seen in Figure 5H. However, we could still dissect six populations of OCPs when looking at CD115 and CD117 expression. Since we were more liberal with what we defined as $CD117^{int}$ we separated CD115/CD117 into four populations.

Despite some of the described trends in macrophage and osteoclast populations, we are largely unable to make significant determinations in treatment-dependent changes in specific cell populations with this particular set of data. This was largely due to the significant variance in frequency within groups. These effects were in part due to the extreme variability in live cell frequency in cancer treated animals. While the sham and naïve animals had cell viabilities within 92-98%, the cancer animals had viabilities anywhere from 18-85%. This also shows the varying levels of tumor establishment and proliferation after cancer surgeries. Because the breast adenocarcinoma cells cannot seed equally between each animal, tumor burden and proliferation are not equal. These variances were exacerbated with small group sizes (N=5). This variability can also be seen with the bone scoring report and lack of significance in the group despite strong preliminary data indicating a high significance in deceases in bone quality between mice treated with saline and mice treated with morphine in both cancer and non-cancer animals (N > 120, data unavailable). We will need to make a few alterations so that we may get substantial results in the future, but this initial data has given us some insight into specific immune cell infiltration with respect to morphine treatment in a CIBP model.

FUTURE DIRECTIONS:

The most important next step is to repeat this experiment using larger treatment groups (N>12). While we prepare for this, we have looked into other modifications that may better fit the overall goal of this project. In preparation for future experiments, we have revisited our immunophenotyping panel in an attempt to expand our view and to label cells with a higher sensitivity and specificity. We propose the following to the gating of macrophages. The standard surface marker for murine macrophages (and monocytes) is F4/80. This is commonly gated against CD11b with double positives indicating undifferentiated macrophages [21,28]. The canonical M1 and M2 polarized macrophage markers are CD11c and CD206, among a few others (CD86 or CD80) [21,25]. However, there are various promising markers that have been explored that can identify more M1s and M2s with higher specificity. Markers such as CD38 for M1s and Egr2 for M2s have promising candidacy in strong and specific identification. Both have shown promising results in specificity and labelling potential. Traditional alternatives such as Arg1 and CD206 for M2s are generally weak due to their shared expression with other cells or their low expression levels. While CD206 can only identify a small fraction of cells, Egr2 has been shown to identify nearly 80% of M2s [28]. Furthermore, we would also like to look into identifying “M2c” phenotypes as they are heavily involved in tissue repair [29]. This cell type would be interesting to see in the context of acute inflammation (sham surgery) and prolonged inflammation (cancer) with respect to morphine treatment. However, little is known about surface expression of M2c macrophages. Strong M1 macrophage markers include iNOS and CD38. Although CD38 is able to label more M1s as compared to iNOS, they also may label some populations of monocytes. So, in the pursuit of specificity, markers such as iNOS and Egr2 will be investigated as potential candidates in identifying M1 and M2 macrophages, respectively.

Additionally, reliably identifying inflammatory monocytes and CMPs/early progenitors is an area of improvement. Based off available antibodies in our panel, we roughly identified

CMPs/MPPs as TN CD11b$^{-/low}$ CD117^{-}/CD115^{+} cells. However, identifying such populations requires very specific markers due to the relatedness of these cells. This is apparent with macrophage and monocyte lineage cells where CD11b, CD11c, and CD68 are expressed in both. We propose the addition of Ly6C, Ly6G and CD14 for (inflammatory) monocyte specific gating [27,30]. CMP/MPP identification is tricky as we have a limited number of antibodies to use in our panel. We will consider markers that are highly specific for cells, with some potential candidates including CXCL12 [31].

Finally, we would like to reexamine RANK's ability to identify osteoclasts. Currently, there is little information regarding whether fully differentiated and mature osteoclasts continue to express this marker. We propose to instead look at markers that are actively expressed and used in osteoclastic activity. Such receptors include Calcitonin R, TRAP, and MMP-9. We can still find value in the RANK receptor, as research has shown using CD14 with RANK can broadly identify pre-osteoclast populations [32].

With such limitations and improvements in mind, we would like to investigate effective markers to better identify current cell populations of interest. We will look into CD38/iNOS for M1 macrophages, Erg2 for M2 macrophages, TRAP/MMP-9/Calcitonin for osteoclasts. In addition, we would like to expand the panel to incorporate the identification of monocytes (using Ly6C, Ly6G, CD11c) and multipotent progenitor/myeloid progenitors (using CD34 and others). We would also prefer to exchange CD19 for B220 as to be more consistent with established protocols towards identifying osteoclast precursors in bone - for our triple-negative gate. It would be interesting to see changes in the TLR-4 receptor frequency in the bone marrow with respect to treatment, as this may provide some insight into the proposed relationship. In the future, we hope that implementing this improved panel with a larger N-value will give us significant data to make power conclusions.

ACKNOWLEDGEMENTS:

I would like to thank my principle investigator Dr. Todd Vanderah and graduate student mentor Austen Thompson at the University of Arizona College of Medicine Department of pharmacology for their close and supportive mentorship on this project. A huge thanks to the Department of Immunobiology for allowing us full access to their LSRFortessa cell counter. I would also like to thank Jen Uhrlaub from Dr. Nikolich-Zulgich's lab as she was always willing to help me develop and run the immunophenotyping panel for flow cytometry.

REFERENCES:

1. Al-Hasani, R. and M. R. Bruchas (2011). "Molecular mechanisms of opioid receptor-dependent signaling and behavior." Anesthesiology 115(6): 1363-1381.
2. McNicol, E., et al. (2003). "Management of opioid side effects in cancer-related and chronic noncancer pain: a systematic review." J Pain 4(5): 231-256.

3. Dursteler-MacFarland, K. M., et al. (2011). "Patients on injectable diacetylmorphine maintenance have low bone mass." Drug Alcohol Rev 30(6): 577-582.
4. Pulido, C., et al. (2017). "Bone metastasis risk factors in breast cancer." Ecancermedicalscience 11: 715.
5. Opioid Painkiller Prescribing, Where You Live Makes a Difference. CDC. 2014. Online.
6. McDonald, J and Lambert DG (2005). "Opioid Receptors." Continuing Education in Anaesthesia Critical Care & Pain 5(1): 22-25.
7. Williams, J. (2008). "Basic Opioid Pharmacology." Rev Pain 1(2): 2-5.
8. Sobczak, M., et al. (2014). "Physiology, signaling, and pharmacology of opioid receptors and their ligands in the gastrointestinal tract: current concepts and future perspectives." J Gastroenterol 49(1): 24-45.
9. Wang, D., et al. (2017). "TLR4 Inactivation in Myeloid Cells Accelerates Bone Healing of a Calvarial Defect Model in Mice." Plast Reconstr Surg 140(2): 296e-306e.
10. Vaure, C. and Y. Liu (2014). "A comparative review of toll-like receptor 4 expression and functionality in different animal species." Front Immunol 5: 316.
11. Hutchinson, M. R., et al. (2010). "Evidence that opioids may have toll-like receptor 4 and MD-2 effects." Brain Behav Immun 24(1): 83-95.
12. Chrastil J., et al. (2013). "Postoperative opioid administration inhibits bone healing in an animal model." Clin Orthop Relat Res 471(12): 4076-4081.
13. Feng, X. and S. L. Teitelbaum (2013). "Osteoclasts: New Insights." Bone Res 1(1): 11-26.
14. Fixe, P. and V. Praloran (1998). "M-CSF: haematopoietic growth factor or inflammatory cytokine?" Cytokine 10(1): 32-37.
15. Xiao, Y., et al. (2013). "Osteoclast precursors in murine bone marrow express CD27 and are impeded in osteoclast development by CD70 on activated immune cells." Proc Natl Acad Sci U S A 110(30): 12385-12390.
16. Boyce, B. F. and L. Xing (2007). "Biology of RANK, RANKL, and osteoprotegerin." Arthritis Res Ther 9 Suppl 1: S1.
17. Arai, F., et al. (1999). "Commitment and differentiation of osteoclast precursor cells by the sequential expression of c-Fms and receptor activator of nuclear factor kappaB (RANK) receptors." J Exp Med 190(12): 1741-1754.
18. Loi, F., et al. (2016). "Inflammation, fracture and bone repair." Bone 86: 119-130.
19. Azuma, Y., et al. (2000). "Tumor necrosis factor-alpha induces differentiation of and bone resorption by osteoclasts." J Biol Chem 275(7): 4858-4864.
20. Takagaki, K., et al. (2012). "Parathyroid hormone-related protein expression, in combination with nodal status, predicts bone metastasis and prognosis of breast cancer patients." Exp Ther Med 3(6): 963-968.
21. Yu, Y. R., et al. (2016). "A Protocol for the Comprehensive Flow Cytometric Analysis of Immune Cells in Normal and Inflamed Murine Non-Lymphoid Tissues." PLoS One 11(3): e0150606.
22. Jacquin, C., et al. (2006). "Identification of multiple osteoclast precursor populations in murine bone marrow." J Bone Miner Res 21(1): 67-77.

23. Jacome-Galarza, C. E., et al. (2013). "Identification, characterization, and isolation of a common progenitor for osteoclasts, macrophages, and dendritic cells from murine bone marrow and periphery." J Bone Miner Res 28(5): 1203-1213.
24. Miyamoto, T., et al. (2001). "Bifurcation of osteoclasts and dendritic cells from common progenitors." Blood 98(8): 2544-2554.
25. Ying, W., et al. (2013). "Investigation of macrophage polarization using bone marrow derived macrophages." J Vis Exp(76).
26. Liu, X. and N. Quan (2015). "Immune Cell Isolation from Mouse Femur Bone Marrow." Bio Protoc 5(20).
27. Italiani, P. and D. Boraschi (2014). "From Monocytes to M1/M2 Macrophages: Phenotypical vs. Functional Differentiation." Front Immunol 5: 514.
28. Jablonski, K. A., et al. (2015). "Novel Markers to Delineate Murine M1 and M2 Macrophages." PLoS One 10(12): e0145342.
29. Mantovani A., et al. (2004). “The chemokine system in diverse forms of macrophage activation and polarization.” Trends Immunol 25(12): 677-686
30. Yang, J., et al. (2014). "Monocyte and macrophage differentiation: circulation inflammatory monocyte as biomarker for inflammatory diseases." Biomark Res 2(1): 1.
31. Kondo, M. (2010). "Lymphoid and myeloid lineage commitment in multipotent hematopoietic progenitors." Immunol Rev 238(1): 37-46.
32. Atkins, G. J., et al. (2006). "RANK Expression as a cell surface marker of human osteoclast precursors in peripheral blood, bone marrow, and giant cell tumors of bone." J Bone Miner Res 21(9): 1339-1349.
33. Gabrilovich, D. I., et al. (2012). "Coordinated regulation of myeloid cells by tumours." Nat Rev Immunol 12(4): 253-268.